Journal of The Electrochemical Society

The Electrochemical Society
Advancing solid state & electrochemical science & technology

Biosensor Encapsulation via Photoinitiated Chemical Vapor Deposition (piCVD)

To cite this article: Ruolan Fan and Trisha L. Andrew 2021 *J. Electrochem. Soc.* **168** 077518

View the article online for updates and enhancements.

This content was downloaded from IP address 96.33.174.43 on 24/10/2022 at 19:19

Journal of The Electrochemical Society, 2021 **168** 077518
1945-7111/2021/168(7)/077518/6/$40.00 © 2021 The Electrochemical Society ("ECS"). Published on behalf of ECS by IOP Publishing Limited

Biosensor Encapsulation via Photoinitiated Chemical Vapor Deposition (piCVD)

Ruolan Fan[1] **and Trisha L. Andrew**[1,2,z]

[1]*Department of Chemistry, University of Massachusetts Amherst, Amherst, Massachusetts, United States of America*
[2]*Department of Chemical Engineering, University of Massachusetts Amherst, Amherst, Massachusetts, United States of America*

Thin and porous poly(hydroxyethyl acrylate) (pHEA) and poly(3,3,4,4,5,5,6,6,7,7,8,8,8-Tridecafluorooctyl acrylate) (pTFOA) encapsulating layers were successfully deposited on model electrical and optical glucose sensors via photoinitiated chemical vapor deposition (piCVD). This surface-restricted chain growth process afforded uniform coverage and strong interfacial adhesion of the resulting polymer encapsulation layers, which enabled the whole sensing area to be fully covered, even after being subjected to numerous electrochemical scanning cycles. Meanwhile, the amorphous films allowed rapid ion and analyte diffusion through themselves and, therefore, achieved quick sensing responses. Especially, pTFOA promised well-defined calibration curves with good repeatability. Furthermore, piCVD films maintained their morphology after being dehydrated and rehydrated over multiple days demonstrating their excellent stability as surface protective layers. These promising features of pHEA and pTFOA synthesized via piCVD may serve as a new encapsulating idea to be applied to various wearable sensors with different substrates and serve as a new strategy to extend the shelf life and functionality of biosensors.
© 2021 The Electrochemical Society ("ECS"). Published on behalf of ECS by IOP Publishing Limited. [DOI: 10.1149/1945-7111/ac1705]

Manuscript submitted May 25, 2021; revised manuscript received July 20, 2021. Published July 30, 2021. *This paper is part of the JES Focus Issue on the 18th International Meeting on Chemical Sensors (IMCS-18)—Volume Two.*

Supplementary material for this article is available online

Personalized physiological monitoring with wearable sensors have received focused attention over the past decade.[1,2] Wearable sensors, particularly wearable electrochemical sensors, whose potential to monitor and respond to the wearer's detailed health signals in real time, are regarded as attractive alternatives to traditional bulky analytical instruments. However, unlike the well-controlled laboratory-based sensors whose analytical performance is largely determined by the active electrode materials, on-body monitoring also requires the sensing system itself to be encapsulated to prevent fouling and retain function under changing microenvironments. Nowadays, wearable sensors with various formats, especially aiming at detecting small biomolecules from body fluids like sweat, have been proposed, such as polymer-based tattoo paper,[3,4] natural cellulose paper[5] and synthetic textiles.[6–8] Although satisfactory selectivity have been achieved by utilizing bioreceptors (enzyme, antibody, aptamer, etc.) among glucose, urea, cortisol, etc sensors,[2] their electrochemical signals suffer from degradation due to fouling and storage under suboptimal conditions, which creates false positives and false negatives. Therefore, a protective layer that preserves the shelf stability and longitudinal function of biosensors is necessary, which can also be easily applied over the many flexible and textured substrates where nascent sensors have been fabricated.

To produce a protective layer or a functional layer for future use without sacrificing the original sensing platform, a substrate-independent and gentle deposition method is required. Besides, to ensure fast signal acquisition, such deposition should also create thin and porous films, which will facilitate mass transfer and analytes diffusion. One such process is chemical vapor deposition (CVD). CVD is a solvent-free process in which vapor-phase precursors chemically react on a substrate surface to generate a thin, solid film.[9] CVD enables in situ polymer synthesis and deposition on arbitrary substrates with tunable microstructure.[10,11] Previous studies have demonstrated that ultrathin hydrogels can be synthesized via photoinitiated chemical vapor deposition (piCVD) on delicate optical sensors without sacrificing sensitivity and accuracy.[12,13] However, few studies[14–17] have been conducted to prove whether such top layers can be integrated into more complicated sensing elements, such as electrochemical biosensors that generate signals via cascade redox reactions.

In current study, the main purpose was to investigate whether piCVD could provide thin enough and firmly attached protective layers and what type of antifouling material is better for electrochemical analysis. Hydrophilic materials[18,19] and zwitterionic polymers[20,21] whose capabilities of facilitating the formation of hydration layers at interface to decrease nontarget analytes permeation have been widely considered in biosensing fields. In this study, a hydrogel film, poly(hydroxyethyl acrylate) (pHEA), was first created via piCVD. HEA was chosen due to its biocompatibility and excellent water retention properties, which can extend the shelf life of biological recognition elements used in many biosensors.[22] Considering that the hydration layer on the pHEA surface might inhibit analyte adsorption at certain potential or within certain potential range, a biocompatible hyperbranched fluoropolymer—poly (3,3,4,4,5,5,6,6,7,7,8,8,8-Tridecafluorooctyl acrylate) (pTFOA)[23]—was also investigated. Hyperbranched fluoropolymers are emerging antifouling encapsulation materials, as they present low surface energies which enable easy removal of bio-macromolecules.[24] Concerns may rise considering that the low wettability of fluorine-containing materials would reduce analyte access as well. However, since partially discontinuous, wrinkled fluoropolymer film can be realized by piCVD process during which multiple monomer nucleation sites with small gaps occurring simultaneously,[23] such questions brought up by materials themselves could be minimized. The surface-restricted polymerization feature of piCVD enabled firmly attached protective layers, which could survive at constant electrical sweeps and swelling/deswelling cycles. Thin and porous films were deposited on well-studied classic enzyme-based electrical and optical glucose sensors to demonstrate proof of concept. The mechanical rigidity and ion permeability of all encapsulating layers facilitated fast electrical response and pTFOA coated biosensors afforded well-defined calibration curves. In the case of encapsulated disposable optical sensor, whose sensing accuracy is determined by color generation/extraction across the whole sensing area, pHEA and pTFOA successfully maintained the bioactivity of enzyme underneath and allowed for analyte diffusion after being fully dehydrated and stored for extended periods of time, thus confirming its potential to extend the shelf life of current biosensors.

Experimental

Materials and reagents.—Glucose oxidase (GOx) (Type X-S, lyophilized powder, 100,000–250,000 units g^{-1} solid), Bovine Serum Albumin (BSA) (lyophilized powder, ⩾96%), 2-hydroxyethyl acrylate (HEA), 2-hydroxy-2-methylpropiophenone (HMPP), chitosan (Chi) (medium molecular weight), potassium ferrocyanide ($K_3[Fe(CN)_6]$),

[z]E-mail: tandrew@umass.edu

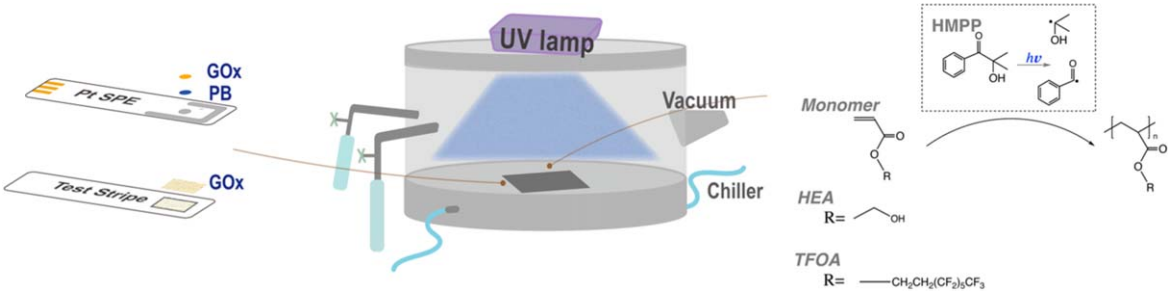

Figure 1. Summary scheme of encapsulating biosensors via piCVD.

iron chloride ($FeCl_3$), 3,3,4,4,5,5,6,6,7,7,8,8,8-Tridecafluorooctyl acrylate (TFOA), potassium phosphate monobasic, sodium phosphate dibasic, sodium chloride, potassium chloride were obtained from Sigma-Aldrich.

Gold quartz crystal sensors (QCM) (5 MHz Au Quartz Crystal Wrap-Around electrode) were purchased from Gamry Instruments, Platinum (Pt) Screen-Printed electrodes (SPE) (2 mm OD circle of working electrode, Ag/AgCl and Pt as reference electrode and counter electrode respectively) were purchased from Pine research. Hydrogen peroxide test stripes (ColorKim, 0–100 ppm range) were obtained by Amazon.

pHEA/pTFOA deposition via piCVD.—A custom-built iCVD chamber (stainless-steel walls, 290 mm diameter, 70 mm height) was used to polymerize HEA (monomer) directly on the surface of all samples. In all experimental runs, a low intensity UV lamp (UVP, UVLS-24 EL Series, 4-Watt, 254 nm) turned on when the monomer flowed into the chamber and the base pressure of the chamber had stabilized. During deposition, the pressure of the reactor was maintained at 200 mTorr, while the stage temperature was controlled at 20 °C through a built-in cooling tube. Photoinitiator and monomer were heated using fiberglass heating tape wrapped around the storage ampules and vaporized into the reactor through needle valves as illustrated in Fig. 1. HMPP was heated at 110 °C and flowed into the chamber first for 5 min, then HEA or TFOA, vaporized at 105 °C, was introduced into the chamber, where it reacted with initiator radicals and polymerized. The deposition was allowed to proceed for 2–5 min to obtain a thin film of 200 nm. After deposition, the samples were aged under vacuum until the temperature of reactants came to room temperature. This post annealing step allowed unreacted monomers to be pulled out of the film, which resulted in a porous coating on the substrate surface. The chemical structure of the piCVD film was determined by Fourier Transform Infrared (FTIR) Spectroscopy (Bruker Alpha P). Thickness and microstructure were investigated via a profilometer (Veeco Dektak Stylus Profilometer).

Preparation of pHEA encapsulated glucose sensor.—In the glucose sensing system, GOx, an enzyme bioreceptor, catalyzes oxidation of glucose and triggers an electron transfer which can be quantified by either current change of an electrochemical sensor or redox-induced color intensity change of an optical sensor.[5] In the current study, we deposited pHEA and pTFOA on both electrochemical and optical glucose sensors.

For electrochemical sensors, a Pt SPE was rinsed with DI water and sonicated in isopropanol, followed by a 15 min plasma treatment to remove surface impurities. An aqueous solution of 100 mM KCl, 2.5 mM $K_3[Fe(CN)_6]$ and 2.5 mM $FeCl_3$ in 100 mM HCl was prepared to deposit Prussian Blue (PB), an electron mediator widely used in biosensing.[2] The Pt SPE was dipped into the solution and applied a voltage swept from −0.15 to 0.3 V vs Ag/AgCl for 4 cycles at a scan rate of 20 mV S^{-1}. After deposition of PB, the electrode was rinsed with DI water and left in a vacuum oven at 80 °C for 1 h. Then the electrode was stabilized by scanning from −0.2 to 0.5 V vs Ag/AgCl at scan rate of 50 mV s^{-1} in 0.1 M phosphate-buffered saline (PBS, pH = 7.4) until a constant cyclic voltammogram was obtained (usually 3 cycles). This modified electrode is denoted as PB-SPE. For optical sensors, the commercial peroxide test stripes were used without any modification.

A solution of 100 U ml^{-1} GOx and 10 mg ml^{-1} BSA was prepared in PBS. Enzyme solution was drop cast on PB-SPE and test stripes with volume of 3 μl and 10 μl respectively (to fully cover the sensing area). After air drying, both sensors were placed inside the piCVD reactor and encapsulated with pHEA or pTFOA. For the test stripe comparison experiment, 1% chitosan solution was prepared by dissolving chitosan in 2% acetic acid[25] and dropping cast onto test stripes with volume of 3 μl.

Characterization of encapsulated sensors.—Gold quartz crystal sensors (5 MHz Au Quartz Crystal Wrap-Around electrode from Gamry Instruments) coated with polymer films (as described above) were used as a gravimetric sensor to test the mechanical stability and ion permeability of the encapsulation layers. Simultaneous cyclic voltammetry and electrogravimetric measurements were carried out using a Gamry Interface 1000B potentiostat equipped with an electrochemical quartz crystal microbalance (eQCM-10 measurement cell). All eQCM experiments were conducted using a three-electrode setup, with a platinum wire as counter electrode and an aqueous Ag/AgCl as reference electrode, while Pt SPE experiments were characterized via a WaveNow potentiostat from Pine Instruments. The color intensity of test stripes was extracted and calculated using Adobe Photoshop. Contact angles were measured using Oneattension from Biolin.

Glucose in sweat ranged from 0.02 mM to 0.6 mM,[26] in the current study, we expanded to 0.8 mM to prove the detection capability of encapsulated biosensors. To achieve clear visualization, 5 μl 1.0 mM glucose was added to test stripes treated by different dehydration times in a vacuum oven with a setting temperature of 40 °C (the highest possible ambient temperature in daily life). All experiment were conducted at least three times to ensure repeatability, partial data were normalized for facilitating comparison.[27]

Results and Discussion

Photoexcited carbonyl species are known to decompose into radicals from readily accessible triplet excited states, which can, in turn, initiate a free-radical polymerization.[17] However, in order to reduce the time over which sensitive enzymatic recognition elements are subjected to vacuum conditions (that may cause dehydration/degradation) and UV light (that may cause photodegradation), we used a stepwise deposition algorithm to enact piCVD. In our piCVD process, HMPP, the photo initiator, was first introduced to the chamber followed by monomers to accelerate polymerization rate. Under UV radiation of low intensity, HMPP decomposes and initializes the polymerization over the excited state lifetime of a carbonyl triplet state. In Fig. 2a, no peak at 1640–1660 cm^{-1} or 3000–3100 cm^{-1}, where the unsaturated carbon-carbon double bond of the acrylate monomer should appear, was observed on pHEA and pTFOA scratched films. The spectrum of pHEA showed a broad absorbance at 3200–3600 cm^{-1}, corresponding to the hydroxyl group peak, and 1725–1730 cm^{-1}, corresponding to the carbonyl stretching peak, meanwhile the characteristic absorbance bands of

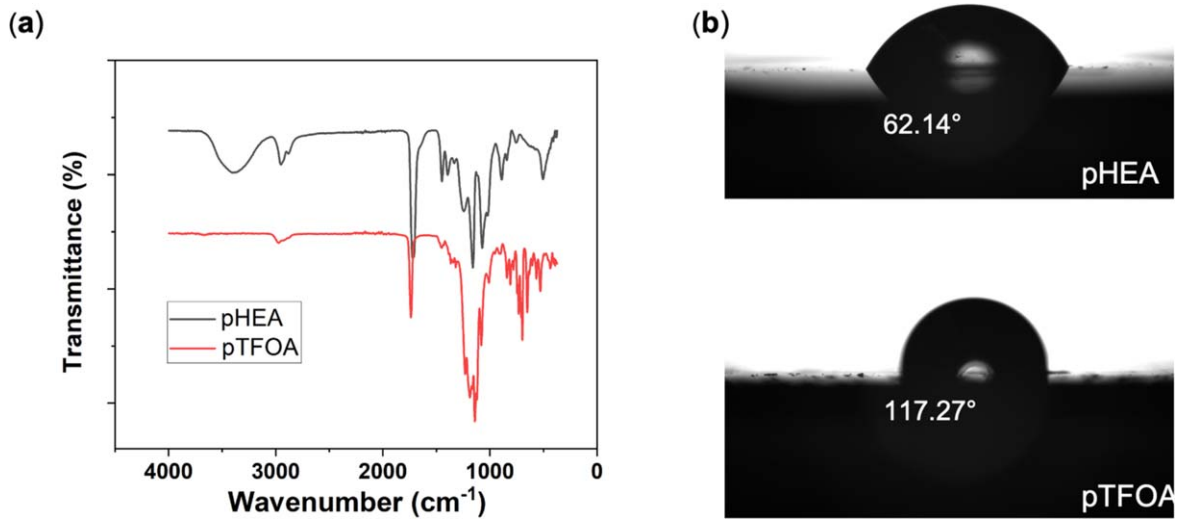

Figure 2. (a) FTIR spectrum of pHEA and pTFOA, (b) water contact angle of pHEA and pTFOA film on silicon wafer.

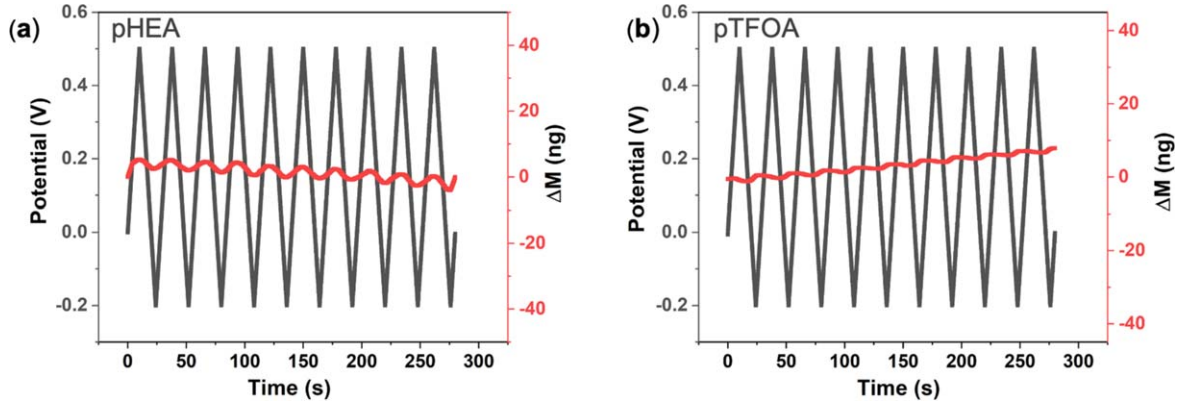

Figure 3. Electrogravimetry traces of (a) pHEA and (b) pTFOA deposited on eQCM in PBS.

CF_2 and CF_3 stretching were observed at 1100–1250 cm^{-1}.[28] In both cases, the FTIR spectrum of films deposited via piCVD verified that the pedant hydroxyl and fluorinated groups, which can serve as self-crosslinking moieties, were retained after the deposition. Besides, due to the overlapping absorbance seen in FTIR, contact angle experiments were conducted on encapsulated silicon wafers to demonstrate the opposite surface feature of two encapsulating films. As shown in Fig. 2b, with the addition of fluorinated branches, pTFOA film exhibited low wettability and thus high contact angle. In contrast, water droplets could easily spread out on pHEA film and showed a contact angle around 60°. The encapsulation layers could still stay on substrates after 10 months stored under air at room temperature as shown in Fig. S1 (available online at stacks.iop.org/JES/168/077518/mmedia).

To perform as a protective layer, it is critical that the film can swell when in aqueous medium while remaining adhered to the sensor substrate.[29] Furthermore, due to the insulating nature of most encapsulation layers, ion and/or electron transport triggered by external potential sweeps can easily cause film delamination.[30] The mechanical durability and permeability of two films via piCVD were examined using an electrochemical quartz crystal microbalance (eQCM). An eQCM measures mass changes occurring at the gold surface with varying and/or cycling applied potentials, allowing us to determine whether a film can firmly adhere to the electrode surface while promising ion exchange between the bulk solution and electrode.[31] Despite the fact that the films were simply physisorbed to the gold (quartz) surface, the randomization of polymer chains (as proved by the broad absorbance seen in Fig. 2a) and surface-restricted growth feature of piCVD allowed a rapid, reversible ion exchange without any noticeable mass loss, as illustrated in Fig. 3. The cyclic voltammogram (CV) of Pt SPE encapsulated by pHEA or pTFOA (pHEA/SPE or pTFOA/SPE) in a solution containing 5 mM ferricyanide/ferrocyanide at varying scan rates from 50 mV s^{-1} to 150 mV s^{-1} were shown in Fig. 4a. The anodic and cathodic peak currents obtained from CV were then plotted as a function of square root of scan rate. The linear change of peak current shown in Fig. 4b with the square root of scan rate and the constant peak potential indicated the redox process was diffusion controlled (we attribute the slight shift seen from pTFOA was due to its low wettability), verifying that these encapsulated films would not interfere with ion and electron transfer.

Classic electrochemical, enzyme-based biosensors have two key components: electron mediator and bioreceptor. Leverage on previous studies,[25–27] electrodeposited PB and drop-cast GOx were chosen as mediator and bioreceptor respectively. The successful PB deposition and material integration was confirmed by cyclic voltammetry in Fig. S2. Although encapsulation serves as a physical barrier which inevitably inhibits charge transfer process, thanks to the thin films obtained via piCVD, redox peaks of PB were still presented after coating. Then, we were able to detect and calibrate glucose by normalizing the recorded data. Glucose oxidation is facilitated by GOx and electrons which are lost from glucose are then captured by electron mediator—PB, as illustrated in Fig. S3. DPV measurements were performed to correlate the electrocatalytic current of PB and the glucose concentration in PBS in the potential range from −0.2 to 0.2 V. Along with the successive addition of glucose, the peak

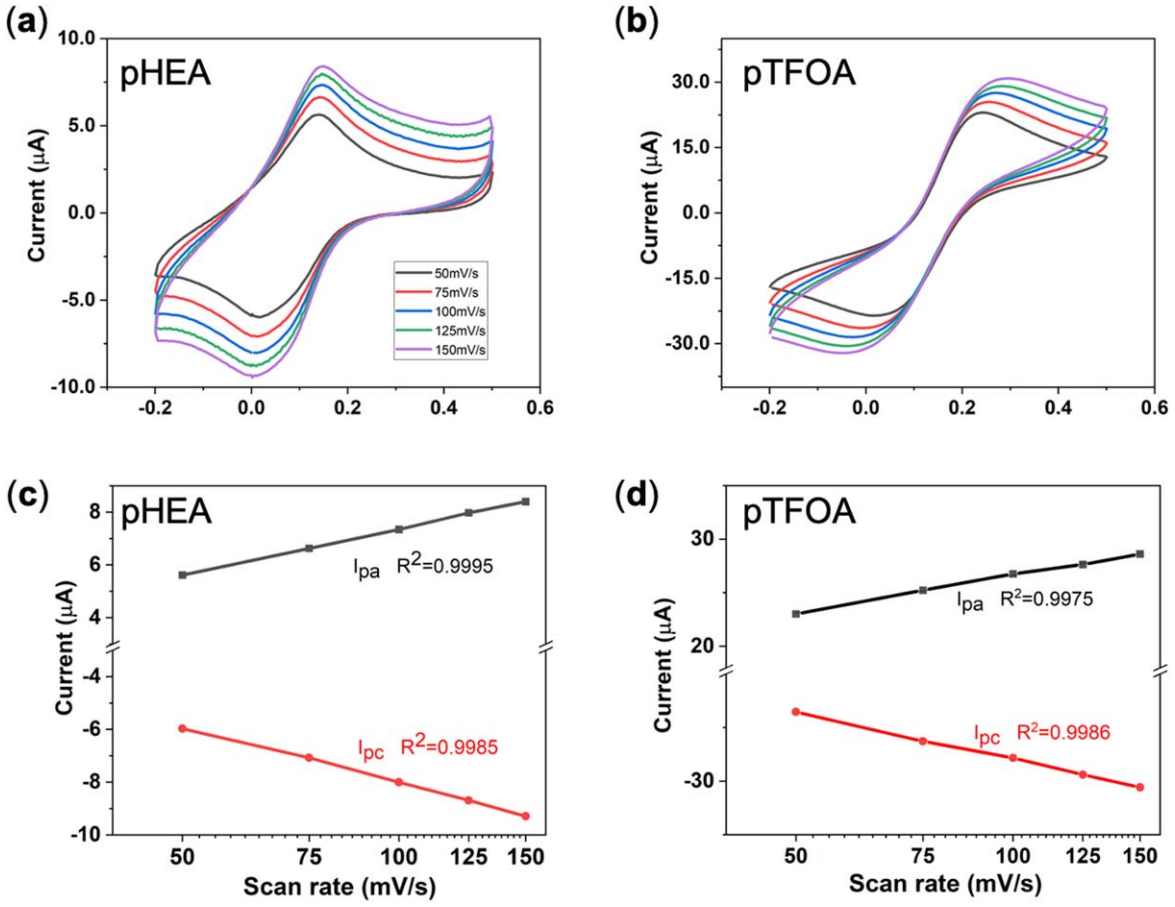

Figure 4. (a) pHEA/SPE and (b) pTFOA/SPE in 5 mM ferricyanide/ferrocyanide at varying scan rates, (c) pHEA/SPE and (d) pTFOA/SPE current to square root of scan rate linear correlation

currents of pTFOA biosensors remained well-defined shape and peak potential, while those of pHEA were slightly changed, as illustrated in Fig. S4. Besides, the two encapsulated sensors showed opposite responses. A biosensor, layered by PB and enzyme but without any encapsulation, was also compared, as shown in Fig. S5. For pHEA/GOx/PB-SPE and GOx/PB-SPE samples, both peak currents decreased correspondingly. The latter can be easily attributed to enzyme loss. When considering pHEA facilitates enzyme immobilization, and those random peak potential swifts occurring during sensing as shown in Fig. S4, the more possible reason would be a resistance increase induced by glucose accumulation on the sensing surface. Although resistance change also gave some linear relationship, as shown in Fig. 5a, the detection range was largely narrowed even in the second run. Thanks to pTFOA hydrophobic nature, pTFOA/GOx/PB-SPE, on the other hand, presented a positive linearity. Note that we stored the pTFOA sensors in PBS for at least 48 h between each cycle, the constant sensitivity (the variation was less than 5%) demonstrated pTFOA has an excellent immobilization and antifouling performance, which are critical for long-term on-site body sensing.

Previous research[27] suggested that constant humidity is a crucial factor for the storage stability of biological recognition elements in biosensors. Here, we intentionally dehydrated coated sensors in a vacuum oven for varying periods of time to understand their moisture retention capability. To easily visualize the coating performance change, peroxide test stripes were used. In the presence

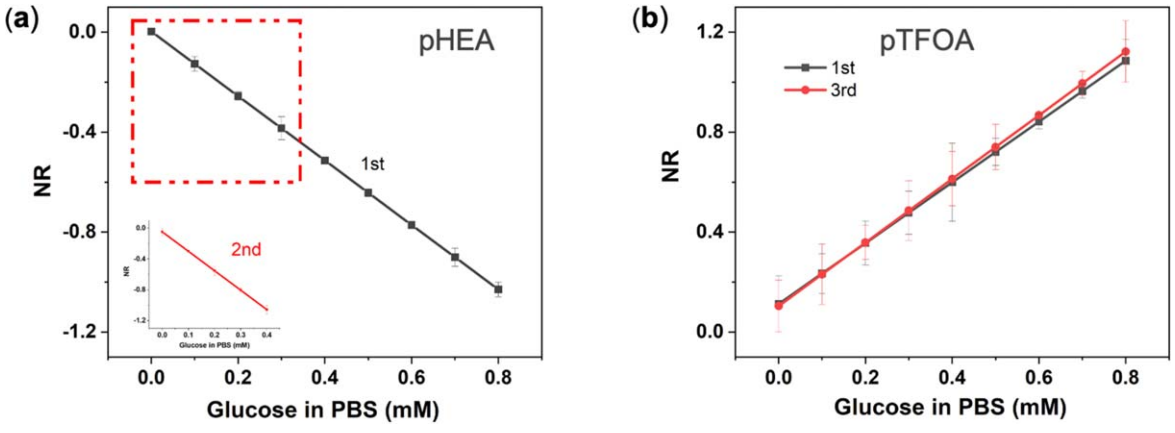

Figure 5. (a) pHEA/GOx/PB-SPE and (b) pTFOA/GOx/PB-SPE calibration curve (NR, normalized response).

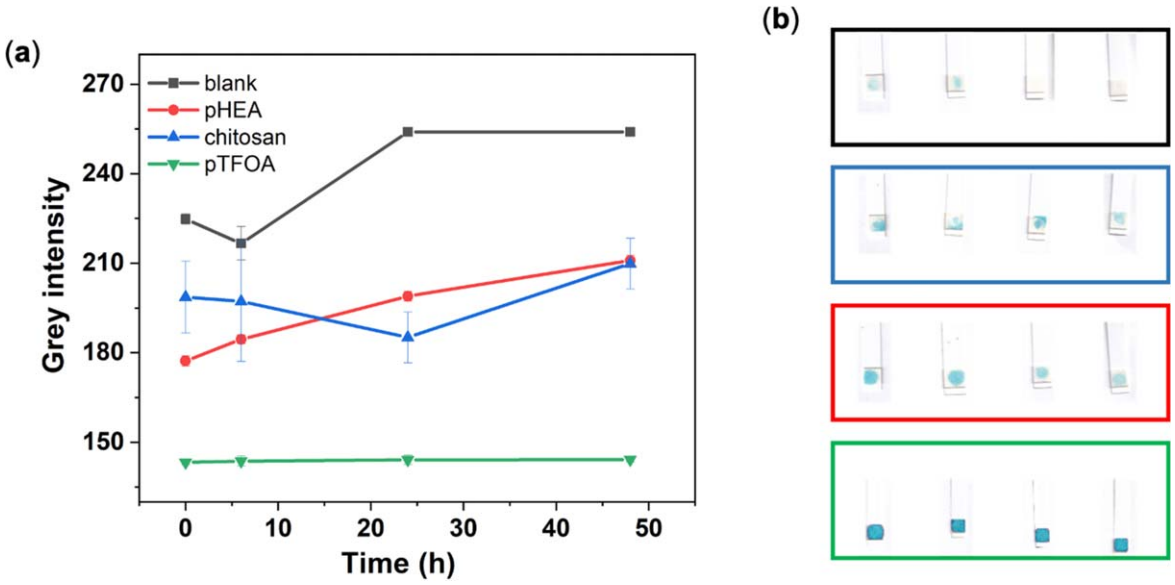

Figure 6. Color intensity changes of encapsulated biosensors under super dry (vacuum) treatment (a) grey intensity and (b) optical format.

of glucose, enzymes initiated a redox reaction and peroxide was produced, which then reacted with the dye on the test stripes and gave a blue color. The darker the blue, the more peroxide generated from either higher glucose concentration or the higher enzyme threshold. Color distribution, which was transformed and presented as an error bar, served as an indication for coating morphology. In Fig. 6a, color change of four series of coated test stripes were investigated. Chitosan was chosen as a control hydrogel, as it is widely used as a solution-deposited protective layer for glucose sensors.[1] Due to the initial color difference resulting from relative humidity in the air and deposition variation, we paid more attention to the absolute color change and error bars. Compared to blank samples, all coated stripes showed relatively low variance in the color intensity after a prolonged vacuum treatment, especially pTFOA coated stripes. The color change of coated test stripes demonstrated that encapsulation films allow for solid state immobilization of GOx (enzyme) without degradation/significant loss which could be possibly caused by salt (from PBS) crystallization during dehydration. Moreover, coatings obtained via piCVD exhibiting a small error bar at each data point indicates that the diffusion pattern was not affected by dehydration. In contrast, chitosan coatings shrunk irreversibly and resulted in a very nonuniform color change over the sensing area as shown in Fig. 6b (morphology change was also demonstrated by obvious contact angle change shown in Fig. S5). As dehydration/varying humidity might become a very critical test when considering sensors' shelf life where any physical and/or chemical variations should be eliminated before the sensing test to ensure the final accuracy, films, particularly hydrophobic ones deposited through piCVD, are strong candidates for biosensing encapsulation.

Conclusions

In this study, we propose a general biosensor encapsulation method via photoinitiated chemical vapor deposition (piCVD). This substrate-agnostic polymerization method can be applied to many wearable sensors, independent of device architecture and sensor complexity and without any hindrance in mass transport. Regarding disposable wearable sensors like test stripes, both pHEA, hydrophilic, and pTFOA, hydrophobic, achieved good enzyme immobilization (maintain bioactivity) when stored in dehydrated conditions. However, during electrochemical sensing, along with the repeating cycles, glucose accumulated on the pHEA surface would cause interference between resistance and amperometric signals. While pTFOA films, because of its hydrophobic nature, could eliminate such issues and therefore serve as an intriguing material for various sensing scenarios.

Acknowledgments

The authors thank Professor Laura Bradley for provising access to her Oneattension contact angle measurement instrument. This work was funded by the National Science Foundation under award CHEM MSN 1807743.

ORCID

Trisha L. Andrew https://orcid.org/0000-0002-8193-2912

References

1. J. R. Sempionatto, I. Jeerapan, S. Krishnan, and J. Wang, *Anal. Chem.*, **92**, 378 (2020).
2. R. Fan and T. L. Andrew, *J. Electrochem. Soc.*, **167**, 037542 (2020).
3. Y. Wang, Y. Qiu, S. K. Ameri, H. Jang, Z. Dai, Y. Huang, and N. Lu, *npj Flex. Electron.*, **2**, 6 (2018).
4. S. Kabiri Ameri, R. Ho, H. Jang, L. Tao, Y. Wang, L. Wang, D. M. Schnyer, D. Akinwande, and N. Lu, *ACS Nano*, **11**, 7634 (2017).
5. C. M. Riccardi, D. Mistri, O. Hart, M. Anuganti, Y. Lin, R. M. Kasi, and C. V. Kumar, *Chem. Commun.*, **52**, 2593 (2016).
6. N. Promphet, P. Rattanawaleedirojn, K. Siralertmukul, N. Soatthiyanon, P. Potiyaraj, C. Thanawattano, J. P. Hinestroza, and N. Rodthongkum, *Talanta*, **192**, 424 (2019).
7. S. Z. Homayounfar, S. Rostaminia, A. Kiaghadi, X. Chen, E. T. Alexander, D. Ganesan, and T. L. Andrew, *Matter*, **3**, 1275 (2020).
8. L. K. Allison and T. L. Andrew, *Adv. Mater. Technol.*, **4**, 1800615 (2019).
9. R. Yang, A. Asatekin, and K. K. Gleason, *Soft Matter*, **8**, 31 (2012).
10. P. Kwong, S. Seidel, and M. Gupta, *ACS Appl. Mater. Interfaces*, **5**, 9714 (2013).
11. G. Dianat, N. Movsesian, and M. Gupta, *ACS Appl. Polym. Mater.*, **2**, 98 (2020).
12. A. Khlyustova, Y. Cheng, and R. Yang, *J. Mater. Chem. B*, **8**, 6588 (2020).
13. G. Ozaydin-Ince, J. M. Dubach, K. K. Gleason, and H. A. Clark, *PANS.*, **108**, 2656 (2011).
14. A. Bérard, G. S. Patience, G. Chouinard, and J. R. Tavares, *Sci Rep.*, **6**, 31574 (2016).
15. K. Chan and K. K. Gleason, *Langmuir*, **21**, 11773 (2005).
16. C. A. Dorval Dion, W. Raphael, E. Tong, and J. R. Tavares, *Surf. Coat. Tech.*, **244**, 98 (2014).
17. S. H. Baxamusa, L. Montero, J. M. Dubach, H. A. Clark, S. Borros, and K. K. Gleason, *Biomacromolecules*, **9**, 2857 (2008).
18. K. Kaewket, C. Karuwan, S. Sonsupap, S. Maensiri, and K. Ngamchuea, *J. Electrochem. Soc.*, **168**, 067501 (2021).
19. A. N. Raditya and D. O'Hare, *J. Electrochem. Soc.*, **167**, 127503 (2020).
20. A. Erfani, J. Seaberg, C. P. Aichele, and J. D. Ramsey, *Biomacromolecules*, **21**, 2557 (2020).
21. S. Paschke and K. Lienkamp, *ACS Appl. Polym. Mater.*, **2**, 129 (2020).

22. S. Z. Homayounfar, A. Kiaghadi, D. Ganesan, and T. L. Andrew, *J. Electrochem. Soc.*, **168**, 017515 (2021).
23. R. Fan, J. Du, K.-W. Park, L. H. Chang, E. R. Strieter, and T. L. Andrew, *ACS Appl. Polym. Mater.*, **3**, 2561 (2021).
24. A. M. C. Maan, A. H. Hofman, W. M. de Vos, and M. Kamperman, *Adv. Funct. Mater.*, **30**, 2000936 (2020).
25. Y. Wang, X. Wang, W. Lu, Q. Yuan, Y. Zheng, and B. Yao, *Talanta*, **198**, 86 (2019).
26. E. Witkowska Nery, M. Kundys, P. S. Jeleń, and M. Jönsson-Niedziółka, *Anal. Chem.*, **88**, 11271 (2016).
27. E. Bihar, S. Wustoni, A. M. Pappa, K. N. Salama, D. Baran, and S. Inal, *npj Flex. Electron.*, **2**, 30 (2018).
28. A. Forner-Cuenca, V. Manzi-Orezzoli, J. Biesdorf, M. E. Kazzi, D. Streich, L. Gubler, T. J. Schmidt, and P. Boillat, *J. Electrochem. Soc.*, **163**, F788 (2016).
29. X. Chen and M. Anthamatten, *Langmuir*, **25**, 11555 (2009).
30. G. Abadias, E. Chason, J. Keckes, M. Sebastiani, G. B. Thompson, E. Barthel, G. L. Doll, C. E. Murray, C. H. Stoessel, and L. Martinu, *J. Vacu. Sci. & Techno. A*, **36**, 020801 (2018).
31. L. Zhang and T. L. Andrew, *Adv. Mater. Interfaces*, **4**, 1700873 (2017).